Correlation between number of ferroelectric variants and coercive field of lead ziconate titanate single crystals

S. Choudhury[a] and L. Q. Chen
Department of Materials Science and Engineering, Penn State University, University Park, Pennsylvania 16802

Y. L. Li
MPA-STC, MS K763, Los Alamos National Lab, Los Alamos, New Mexico 87545 and Department of Materials Science and Engineering, Penn State University, University Park, Pennsylvania 16802

(Received 8 May 2007; accepted 24 June 2007; published online 18 July 2007)

Understanding the magnitude of coercive fields, the external electric field that results in zero net polarization, has been a long-standing problem for ferroelectrics. The authors studied the switching and coercive fields using a combination of the continuum phase field approach, microelasticity, and electrostatics. While the values of coercive fields predicted from the phenomenological thermodynamic theory assuming a single ferroelectric domain or the theory of nucleation are at least one order of magnitude too high compared to those measured experimentally, the predictions incorporating structural inhomogeneities show remarkably good agreement with experimental measurements, revealing the critical role of multidomain/variants in polarization switching. © *2007 American Institute of Physics*. [DOI: 10.1063/1.2759274]

A common feature for all ferroelectrics is the formation of domains upon cooling below the ferroelectric transition temperature. Each domain is a spatial region of uniform spontaneous polarization. The coercive field is defined as the magnitude of an external electric field, which results in zero net polarization. Theoretically, the coercive field calculated from a phenomenological thermodynamic theory assuming a perfect crystal with a single domain corresponds to the critical field that drives a homogeneously polarized ferroelectric to instability. The values of coercive field predicted from such an approach is typically one or more orders of magnitude too high compared to those measured experimentally.[1] On the other hand, Landauer[2] showed that it was impossible to nucleate domains through the homogeneous nucleation mechanism; the estimated nucleation energy barrier ($\sim 10^8$ kT) at an electric field of 1 kV/cm is much too high compared to the available thermal energy. Therefore, to explain the experimentally measured coercive fields, various material inhomogeneities[3–8] have been suggested to be responsible for lowering the domain nucleation barrier, including surfaces, grain boundaries, dislocations, and dipolar defects. For example, it has been shown that structural and/or dipolar defects can reduce the energy barrier for domain nucleation during polarization switching, and thus lead to a much smaller coercive field than thermodynamic estimates.[2,3,9–11] While it is realistic to expect the coercive field of a ferroelectric to be dependent on the defect and defect densities, the existence of defects alone is not sufficient to explain experimentally observed coercive field and the disagreement in the coercive fields between theory and experiments. For example, the experimentally reported coercive fields for a given ferroelectric are within a relatively narrow range, e.g., 9–20 kV cm^{-1} for $PbZr_{1-x}Ti_xO_3$ (PZT) polycrystal at the morphotropic phase boundary (MPB) composition.[12–14] If structural or dipolar defects are the critical structural features that control the coercive field, one would expect much larger variations of coercive fields measured on ferroelectric samples prepared under different processing conditions but with the same chemistry since defect densities are expected to be strongly processing dependent. On the other hand, in the absence of external constraints, the number of ferroelectric domain variants for a ferroelectric is solely determined by the transformation crystallography and is independent of processing conditions, where a variant is defined by the direction of the spontaneous polarization along a definite crystallographic direction. The main focus of this letter is to discuss the relationship between the number of domain variants in a ferroelectric domain structure and the magnitude of coercive fields in an attempt to shed light on the main factors that determine the coercive field.

We consider bulk $PbZr_{1-x}Ti_xO_3$ (PZT) single crystals as the model system for phase field simulations. We employ two-dimensional (2D) and three-dimensional (3D) phase field simulations as well as thermodynamic calculations. Phase field approach has previously been used to predict ferroelectric transition temperatures and domain structures in bulk ferroelectric and thin films.[15–17] Unlike the thermodynamic approach, the phase-field approach does not make any *a priori* assumptions with regard to the possible domain structure that might appear under a given condition. It is able to predict the detailed domain structures and their temporal evolution when a uniform external electric field is applied.[17] In this work, we will demonstrate that with the systematic increase of the number of ferroelectric variants, the predicted coercive field approaches the experimental measurements.

To describe a proper ferroelectric transition, the spontaneous polarization $\mathbf{P}=(P_1,P_2,P_3)$ is chosen as the order parameter. The total free energy of an inhomogeneous ferroelectric single crystal is given by

$$F=\int_V (f_{\text{bulk}}+f_{\text{elas}}+f_{\text{grad}}+f_{\text{elec}})dV, \tag{1}$$

where f_{bulk} is the bulk free energy density, f_{elas} is the elastic energy density, f_{grad} is the gradient energy density which is

[a]Electronic mail: sxc398@psu.edu

only nonzero around domain walls, and f_{elec} is the electrostatic energy density. V is the volume of the simulated system.

The bulk free energy density as a function of polarization was modeled by Haun *et al.*[18] using a six-order polynomial in polarization and given in Ref. 17.

The elastic energy density is calculated by

$$f_{\text{elas}} = \tfrac{1}{2} C_{ijkl} e_{ij} e_{kl} = \tfrac{1}{2} C_{ijkl} (\varepsilon_{ij} - \varepsilon_{ij}^0)(\varepsilon_{kl} - \varepsilon_{kl}^0), \tag{2}$$

where C_{ijkl} is the elastic stiffness tensor, $e_{ij} = \varepsilon_{ij} - \varepsilon_{ij}^0$ is the elastic strain, ε_{ij} is the total strain of the crystal compared to the parent paraelectric phase, and ε_{ij}^0 is the stress-free strain or transformation strain: $\varepsilon_{ij}^0 = Q_{ijkl} P_k P_l$, where Q_{ijkl} is the electrostrictive coefficient. Here we decompose the total strain ε_{ij} as a sum of spatially independent homogenous strain, $\bar{\varepsilon}_{ij}$, and a spatially dependent heterogeneous strain, $\delta\varepsilon_{ij}$, i.e.,

$$\varepsilon_{ij} = \bar{\varepsilon}_{ij} + \delta\varepsilon_{ij}. \tag{3}$$

The calculation of the heterogeneous strain $\delta\varepsilon_{ij}$ is described in details in Ref. 17. The heterogeneous strain is defined by $\int_V \delta\varepsilon_{ij} dV = 0$ so that the homogenous strain determines the macroscopic shape deformation of the single crystal due to an applied strain, phase transformations, or domain structure changes. For example, if the system is clamped, then $\bar{\varepsilon}_{ij}$ is zero. The mathematical expressions for the gradient energy density are given Ref. 17.

Under an applied electric field, the electrostatic energy density f_{elec} consists of three contributions, i.e., the dipole-dipole interaction energy density f_{dipole}, the depolarization energy density f_{depol}, and the energy density due to the applied electric field f_{appel}, i.e.,

$$f_{\text{elec}} = f_{\text{dipole}} + f_{\text{depol}} + f_{\text{appel}}. \tag{4}$$

Detailed method of calculating the electrical energy density was described in our previous paper.[17]

The temporal evolution of the polarization field from nonequilibrium to equilibrium is described by the time-dependent Ginzburg-Landau equation,

$$\frac{\partial P_i(\mathbf{r},t)}{\partial t} = -L \frac{\delta F}{\delta P_i(\mathbf{r},t)} \quad (i = 1,2,3), \tag{5}$$

where L is a kinetic coefficient related to the domain movement. Equation (5) can be numerically solved with the semi-implicit Fourier spectral method.[19]

In the simulations, we discretized the simulation cell as $256\Delta x_1 \times 256\Delta x_2 \times 1\Delta x_3$ and $128\Delta x_1 \times 128\Delta x_2 \times 128\Delta x_3$ grid points. Periodic boundary conditions are applied along the all x_1, x_2 and x_3 directions. The grid spacing was chosen to be $\Delta x_1 = \Delta x_2 = \Delta x_3 = l_0$, where $l_0 = \sqrt{G_{110}/\alpha_0}$ and $\alpha_0 = |\alpha_1|_{T=25\,^\circ\text{C}}$. We assumed that the gradient energy coefficient was $G_{11}/G_{110} = 0.6$ which resulted in a domain wall width about $1.5\Delta x_1$. The time step in Eq. (5) was taken as $\Delta t/t_0 = 0.05$, where $t_0 = 1/(\alpha_0 L)$. For elastic energy calculation, we assumed the elastic constants to be homogenous and isotropic with shear modulus $\mu = 0.476 \times 1011$ N m^{-2} and Poisson's ratio $\nu = 0.312$. Clamped boundary condition was used. For the dipole-dipole interaction energy calculations, $\kappa_{11} = \kappa_{22} = 100$ was used, where κ_{ij} is the relative dielectric permittivity, assumed to be independent of space.

In order to construct a polarization versus applied electric field (PE) loop, an initial domain structure was generated by performing the simulations without an applied electric field, starting from a paraelectric state with small random perturbations. Depolarizing fields along all x_1, x_2, and x_3 directions were considered. Then, an electric field is applied to the domain structure along the x_1 direction while depolarizing fields were assumed to exist along the other x_2 and x_3 directions. At each increment of the electric field, the domain structure from a previous simulation was used as the input, where the increment in the electric field between two consecutive points in the PE loop is maintained at 0.001 kV/cm.

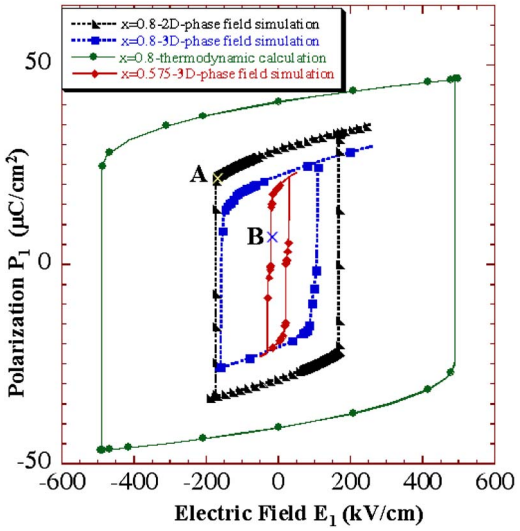

FIG. 1. (Color online) Hysteresis loops for bulk PZT single crystal of composition $x=0.80$ and $x=0.575$. The black and the blue dotted lines are the hysteresis loops obtained from 2D and 3D phase-field simulations for PZT ($x=0.80$) bulk single crystal, respectively. For comparison, the hysteresis loop obtained from thermodynamic calculation assuming a single domain is presented, as shown by green solid line. The red solid line shows the hysteresis loop obtained from a 3D phase-field simulation for PZT ($x=0.575$) bulk single crystal.

As the first example, PZT with composition of $x=0.80$ was considered. Its stable ferroelectric phase is of tetragonal symmetry. The polarization versus PE loops obtained in the 2D and 3D simulations were given by dotted lines in Fig. 1. In the 2D simulations, the domain structure consists of four possible tetragonal variants, namely, a_1 positive, a_2 positive, a_1 negative, and a_2 negative, with polarization components $(P_1>0, P_2=P_3=0)$, $(P_2>0, P_1=P_3=0)$, $(P_1<0, P_2=P_3=0)$, and $(P_2<0, P_1=P_3=0)$, respectively. In the 3D simulations, a domain structure may have all its six possible tetragonal variants, i.e., in addition to those present in 2D, a_3 positive and a_3 negative with polarization components $(P_1=P_2=0, P_3>0)$ and $(P_1=P_2=0, P_3<0)$ are included. As shown in Fig. 1 the predicted coercive field of 131.7 kV cm^{-1} in 3D is less than that (170.54 kV cm^{-1}) obtained in 2D. The decrease in the predicted coercive field in 3D as compared to 2D can be attributed to the additional two tetragonal variants. For comparison, the hysteresis loop obtained from the thermodynamic calculation under a single tetragonal domain assumption is shown by the green solid line in the same figure. It is seen that the coercive field from the thermodynamic calculation is about three and half times large as that obtained from the 3D phase field simulation. Based on the hysteresis loops for PZT ($x=0.80$) single crystals obtained from the thermodynamic calculation, 2D and 3D phase field simulations, we make a hypothesis that the coercive field of a ferroelectric is closely related to the num-

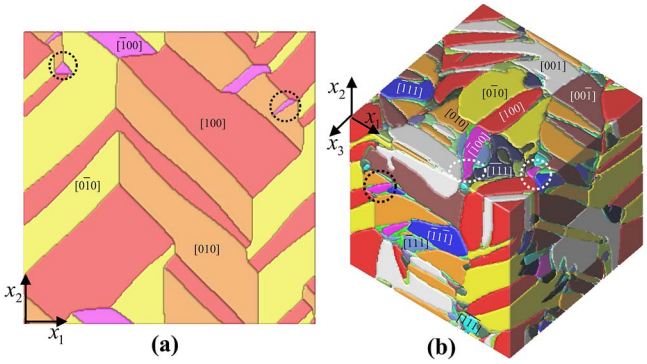

FIG. 2. (Color online) Domain structures obtained from phase field simulations during domain switching. The polarization directions of the ferroelectric variants are indicated. (a) Domain structure of a PZT ($x=0.80$) single crystal corresponding to point A in Fig. 1 from the 2D simulation. Areas marked by circles show that the a_1 negative domains nucleate at the twin boundaries. (b) Domain structure corresponding to point B in Fig. 1 for a PZT single crystal with composition of $x=0.575$ from the 3D simulation. The blue colors represent rhombohedral phase while the rest of the colors represent tetragonal variants. Areas marked by the circles show the nucleation locations of tetragonal a_1 negative variant during switching.

ber of ferroelectric domain variants. The predicted coercive field decreases as the number of variants increases for the same system.

To test this hypothesis, we performed additional 3D phase field simulations of PZT single crystals near the morphotropic phase boundary. In this case, it is possible to have all six tetragonal variants as well as eight rhombohedral variants for a total of fourteen variants in the domain structure.[20] The red solid line in Fig. 1 is the corresponding hysteresis loop. Quite remarkably, the coercive field is dramatically reduced, approximately 20.05 kV cm^{-1}, which is about one-seventh of that for the tetragonal ferroelectric state of PZT at $x=0.80$ predicted by the 3D simulation.

To understand the role of the number of domain variants in reducing the coercive field, we examined the domain structure evolution during switching. Figure 2(a) is a 2D domain structure corresponding to point A in Fig. 1. Each color represents a tetragonal variant and the direction of the polarization is indicated for each variant. It is shown that a_1 negative domains nucleate at the twin boundaries, i.e., 90° domain walls (marked by the circles). Figure 2(b) is a domain structure from a 3D simulation of PZT at the MPB composition ($x=0.575$), corresponding to point B in Fig. 1. The domain structure contains a phase mixture. Rhombohedral ferroelectric variants are represented by different blue shades, while other colors denote the tetragonal variants. It is demonstrated that a_1 negative domains nucleate either at the domain boundaries between tetragonal and rhombohedral variants or at the boundaries between different tetragonal variants (marked by circles) during switching. Comparing the 2D and 3D domain structures, the significantly reduced coercive field at the MPB composition can be mostly attributed to the increase in the number of ferroelectric variants as compared to the tetragonal composition.

The experimentally measured coercive fields for tetragonal compositions and for compositions near the MPB are 22–40 (Refs. 21–23) and 9–20 kV cm^{-1} (Refs. 12–14), respectively. The predicted coercive fields for single crystals obtained from our 3D phase field simulations for compositions of $x=0.80$ and $x=0.575$ are about three to six times and one to two times the experimental measurements while the predicted coercive field assuming a single tetragonal domain is 11–20 times the experimental measurements. It should be pointed out that the experimentally measured hysteresis loops for PZT are for polycrystalline samples. Therefore, the additional difference in the simulated coercive fields and experimental measurements is possibly due to the presence of defects such as grain boundaries and dislocations present in polycrystalline ceramics. The role of these extrinsic defects becomes increasingly important as the number of ferroelectric variants decreases. Theoretical models are now available[17,24] for introducing defects such as dislocations as well as grain structures, and it has been shown that they will likely further reduce the predicted coercive field.

In conclusion, the presence of multivariants/multidomains accounts for the dramatically different values of coercive fields of bulk ferroelectric crystals predicted from prior phenomenological thermodynamic theory. It is shown that the nucleation of domains during polarization switching occurs at the domain walls among various ferroelectric domains in a single crystal.

The financial support from NSF under Grant Nos. DMR-0507146 and DMR-0213623 is gratefully acknowledged.

[1] H. F. Kay and J. W. Dunn, Philos. Mag. **7**, 2027 (1962).
[2] R. Landauer, J. Appl. Phys. **28**, 227 (1957).
[3] A. M. Bratkovsky and A. P. Levanyuk, Phys. Rev. Lett. **85**, 4614 (2000).
[4] J. F. Scott, J. Phys.: Condens. Matter **18**, R361 (2006).
[5] G. Gerra, A. K. Tagantsev, and N. Setter, Phys. Rev. Lett. **94**, 107602 (2005).
[6] A. Roelofs, N. A. Pertsev, R. Waser, F. Schlaphof, L. M. Eng, C. Ganpule, V. Nagarajan, and R. Ramesh, Appl. Phys. Lett. **80**, 1424 (2002).
[7] C. S. Ganpule, A. L. Roytburd, V. Nagarajan, B. K. Hill, S. B. Ogale, E. D. Williams, R. Ramesh, and J. F. Scott, Phys. Rev. B **65**, 014101 (2002).
[8] S. Kim, V. Gopalan, K. Kitamura, and Y. Furukawa, J. Appl. Phys. **90**, 2949 (2001).
[9] S. Ducharme, V. M. Fridkin, A. V. Bune, S. P. Palto, L. M. Blinov, N. N. Petukhova, and S. G. Yudin, Phys. Rev. Lett. **84**, 175 (2000).
[10] M. E. Drougard, R. Landauer, and D. R. Young, Phys. Rev. **98**, 1010 (1955).
[11] M. I. Molotskii and M. M. Shvebelman, Philos. Mag. **85**, 1637 (2005).
[12] L. B. Kong and J. Ma, Mater. Lett. **51**, 95 (2001).
[13] L. B. Kong, J. Ma, R. F. Zhang, W. Zhu, and O. K. Tan, Mater. Lett. **55**, 370 (2002).
[14] A. Y. Wu, P. M. Vilarinho, I. M. M. Salvado, and J. L. Baptista, J. Am. Ceram. Soc. **83**, 1379 (2000).
[15] S. Choudhury, Y. L. Li, and L. Q. Chen, J. Am. Ceram. Soc. **88**, 1669 (2005).
[16] Y. L. Li, S. Y. Hu, Z. K. Liu, and L. Q. Chen, Acta Mater. **50**, 395 (2002).
[17] S. Choudhury, Y. L. Li, C. E. Krill, and L. Q. Chen, Acta Mater. **53**, 5313 (2005).
[18] M. J. Haun, E. Furman, S. J. Jang, and L. E. Cross, Ferroelectrics **99**, 13 (1989).
[19] L. Q. Chen and J. Shen, Comput. Phys. Commun. **108**, 147 (1998).
[20] J. Y. Li, R. C. Rogan, E. Ustundag, and K. Bhattacharya, Nat. Mater. **4**, 776 (2005).
[21] M. J. Hoffmann, M. Hammer, A. Endriss, and D. C. Lupascu, Acta Mater. **49**, 1301 (2001).
[22] J. Tartaj, C. Moure, L. Lascano, and P. Duran, Mater. Res. Bull. **36**, 2301 (2001).
[23] *Numerical Data and Fundamental Relationships in Science and Technology* (Springer, Berlin, 1981), Vol. 16 III, p. 430.
[24] Y. U. Wang, Y. M. M. Jin, and A. G. Khachaturyan, J. Appl. Phys. **92**, 1351 (2002).